

**Synthesis, Single-Crystal X-ray Microdiffraction,  
 and NMR Characterizations of the Giant Pore  
 Metal-Organic Framework Aluminum Trimesate  
 MIL-100**

Christophe Volkringer,<sup>†</sup> Dimitry Popov,<sup>§</sup>  
 Thierry Loiseau,<sup>\*,†</sup> Gérard Férey,<sup>†</sup>  
 Manfred Burghammer,<sup>§</sup> Christian Riekel,<sup>§</sup>  
 Mohamed Haouas,<sup>‡</sup> and Francis Taulelle<sup>‡</sup>

<sup>†</sup> Porous Solid Group and <sup>‡</sup> Tectospin, Institut  
 Lavoisier—UMR CNRS 8180, Université de Versailles Saint  
 Quentin, 45 avenue des Etats-Unis, 78035 Versailles cedex,  
 France, and <sup>§</sup> ESRF, 6, rue Jules Horowitz, B.P. 220, 38043  
 Grenoble cedex, France

Received July 3, 2009  
 Revised Manuscript Received October 8, 2009

This contribution deals with the hydrothermal synthesis of the metal-organic framework aluminum trimesate, analogous to the MIL-100-type, previously reported with chromium(III) and iron(III). MIL-100(Al) crystallizes within a very narrow pH range (0.5–0.7) after heating a mixture of aluminum nitrate, trimethyl 1,3,5-benzenetricarboxylate (Me<sub>3</sub>btc), nitric acid, and water at 210 °C for 3.5 h. The resulting product consists of tiny octahedral shaped crystals of 2 μm size, which have been used for the atomic structure determination. It was carried out by means of single crystal using the microdiffraction setup together with microfocalized synchrotron radiation at station ID13 (ESRF, France). Solid-state NMR characterization was fully consistent with XRD structure but with higher local symmetry. The three-dimensional open framework obtained from direct methods calculations reveals the arrangement of supertetrahedral (ST) building blocks based on the MTN topology (related to the zeolite ZSM-39). Each ST motif is built up from four μ<sub>3</sub>-oxo-centered trinuclear unit (Al<sub>3</sub>O) located at each corner and linked to the four btc ligands located on each face of the tetrahedron. MIL-100 (Al) exhibits BET and Langmuir surface area of 2152(39) m<sup>2</sup> g<sup>-1</sup> and 2919(44) m<sup>2</sup> g<sup>-1</sup>, respectively (pore volume: 0.82 cm<sup>3</sup> g<sup>-1</sup>).

For the past decade, the class of crystalline metal-organic frameworks (MOF) materials has attracted growing attention due to the occurrence of their fascinating porous infinite networks.<sup>1–4</sup> These hybrid organic–inorganic compounds exhibit rather low-dense and relatively robust three-dimensional architectures delimiting systems of well-defined cavities and/or tunnels and they offer new potential applications in the field of gas

storage, molecular separation, catalysis, drug delivery, and ionic conductors.<sup>1,5</sup> These specific frameworks are usually based on the combination of metallic centers connected with rigid aromatic linkers such as benzene-polycarboxylates. Beside the variety of organic species (length, geometry, number of functionalities, etc.), several connection modes of the inorganic cations have been observed in the chemistry of metal carboxylates, which could define different oligomeric building blocks such as square planar (for example paddle-wheel), tetrahedral, octahedral or trigonal prismatic motifs,<sup>2</sup> chains, or even planes and 3D arrangements.

The trigonal trimer, corresponding to the μ<sub>3</sub>-oxo-centered trinuclear metal cluster, has received special attention because it was encountered as a building unit for the formation of the giant pore compounds of the mesoporous series MIL-100,<sup>6</sup> MIL-101,<sup>7</sup> and flexible hybrid frameworks MIL-88<sup>8</sup> with very large swelling effect. The existence of isolated metallic trimers is well-documented in the literature for the transition metals<sup>9</sup> and was also observed in MOF-type compounds with the divalent cations nickel<sup>10,11</sup> or zinc<sup>12</sup> and trivalent cations scandium,<sup>13</sup> vanadium,<sup>14</sup> chromium,<sup>6–8,15</sup> or iron.<sup>16–18</sup> More recently, such a unit was also reported in MOF phases incorporating the p elements, such as aluminum,<sup>19</sup> gallium,<sup>20</sup> and indium.<sup>21,22</sup> However, the formation of such a trinuclear metallic block is still challenging for aluminum when compared to the transition metals. Its occurrence

\*Corresponding author. E-mail: thierry.loiseau@ensc-lille.fr.

(1) Férey, G. *Chem. Soc. Rev.* **2008**, *37*, 191.  
 (2) Yaghi, O. M.; O'Keeffe, M.; Ockwig, N. W.; Chae, H. K.; Eddaoudi, M.; Kim, J. *Nature* **2003**, *423*, 705.  
 (3) Moulton, B.; Zaworotko, M. J. *Chem. Rev.* **2001**, *101*, 1629.  
 (4) Kitagawa, S.; Kitaura, R.; Noro, S.-I. *Angew. Chem., Int. Ed.* **2004**, *43*, 2334.

(5) Janiak, C. *Dalton Trans.* **2003**, 2781.  
 (6) Férey, G.; Serre, C.; Mellot-Draznieks, C.; Millange, F.; Surblé, S.; Dutour, J.; Margiolaki, I. *Angew. Chem., Int. Ed.* **2004**, *43*, 6296.  
 (7) Férey, G.; Mellot-Draznieks, C.; Serre, C.; Millange, F.; Dutour, J.; Surblé, S.; Margiolaki, I. *Science* **2005**, *309*, 2040.  
 (8) Serre, C.; Mellot-Draznieks, C.; Surblé, S.; Audebrand, N.; Filinchuck, Y.; Férey, G. *Science* **2007**, *315*, 1828.  
 (9) Cotton, F. A.; Wilkinson, G. In *Advanced Inorganic Chemistry*, 5th ed.; John Wiley & Sons: New York, 1988.  
 (10) Jia, J.; Lin, X.; Wilson, C.; Blake, A. J.; Champness, N. R.; Hubberter, P.; Walker, G.; Cussen, E. J.; Schröder, M. *Chem. Commun.* **2007**, 840.  
 (11) Ma, S.; Wang, X.-S.; Manis, E. S.; Collier, C. D.; Zhou, H.-C. *Inorg. Chem.* **2007**, *46*, 3432.  
 (12) Seo, J. S.; Whang, D.; Lee, H.; Jun, S. I.; Oh, J.; Jeon, Y. J.; Kim, K. *Nature* **2000**, *404*, 982.  
 (13) Dietzel, P. D. C.; Blom, R.; Fjellvag, H. *Dalton Trans.* **2006**, 2055.  
 (14) Barthelet, K.; Riou, D.; Férey, G. *Chem. Commun.* **2002**, 1492.  
 (15) Surblé, S.; Millange, F.; Serre, C.; Düren, T.; Latroche, M.; Bourrelly, S.; Llewellyn, P. L.; Férey, G. *J. Am. Chem. Soc.* **2006**, *128*, 14889.  
 (16) Serre, C.; Millange, F.; Surblé, S.; Férey, G. *Ang. Chem., Int. Ed.* **2004**, *43*, 6285.  
 (17) Horcajada, P.; Surblé, S.; Serre, C.; Hong, D.-Y.; Seo, Y.-K.; Chang, J.-S.; Grenèche, J.-M.; Margiolaki, I.; Férey, G. *Chem. Commun.* **2007**, 2820.  
 (18) Sudik, A. C.; Côté, A. P.; Yaghi, O. M. *Inorg. Chem.* **2005**, *44*, 2998.  
 (19) Loiseau, T.; Lecroq, L.; Volkringer, C.; Marrot, J.; Férey, G.; Haouas, M.; Taulelle, F.; Bourrelly, S.; Llewellyn, P. L.; Latroche, M. *J. Am. Chem. Soc.* **2006**, *128*, 10223.  
 (20) Volkringer, C.; Loiseau, T.; Férey, G.; Morais, C.; Taulelle, F.; Montouillout, V.; Massiot, D. *Microporous Mesoporous Mater.* **2007**, *105*, 111.  
 (21) Volkringer, C.; Loiseau, T. *Mater. Res. Bull.* **2006**, *41*, 948.  
 (22) Liu, Y.; Eubank, J. F.; Cairns, A. J.; Eckert, J.; Kravtsov, V. C.; Luebke, R.; Eddaoudi, M. *Angew. Chem., Int. Ed.* **2007**, *46*, 3278.

was described only recently by Roesky<sup>23</sup> and Bekaert<sup>24</sup> as isolated molecular cluster with acetate ligands. The existence of the trinuclear oxo-centered prototype in the aluminum trimesate MIL-96<sup>19</sup> opens the way to design structures analogous to the MIL-100/101 topologies. The choice of aluminum for making MOF-type compounds is based on different considerations. As a light element, relatively low density materials can be obtained and solids with high gas storage capacity can be investigated. Moreover, as a cheap metal, aluminum-based material could be produced at relatively low cost at the industrial scale.<sup>25,26</sup>

We therefore investigated the chemical system involving aluminum and the trimesate (or btc or 1,3,5-benzenetricarboxylate) ligand in order to reproduce the synthesis of MIL-100 network, which was previously obtained with chromium<sup>7</sup> or iron.<sup>17</sup>

Many difficulties arose from the complexity of this system in order to isolate pure phases. Indeed, pH represents an important and subtle parameter of the syntheses. Depending on it, two porous aluminum trimesates have been previously isolated. The phase MIL-96<sup>19</sup> is formed at pH values varying from 1 to 3 after 24 h, whereas MIL-110<sup>27</sup> appears in very acidic conditions (pH ~0–0.3) after heating at 210 °C for 72 h (or at pH 3.5–4.0, but after heating for only 3 h<sup>28</sup>). During the course of our work, we observed the formation of the aluminum-based MIL-100 trimesate  $(\text{Al}_3\text{O}(\text{OH})(\text{H}_2\text{O})_2[\text{btc}]_2 \cdot n\text{H}_2\text{O})$ , at very short reaction times (3–4 h) in a very narrow range of pH (0.5–0.7) from a mixture of aluminum nitrate, trimethyl 1,3,5-benzenetricarboxylate, nitric acid, and water.<sup>29</sup> Out to these specific synthesis conditions, a mixture of MIL-96/MIL-110 is always observed. SEM analysis of MIL-100 (Al) indicated the occurrence of tiny single crystals with a typical octahedral shape of 0.5–2  $\mu\text{m}$  size (Figure 1).

For the X-ray diffraction experiment, this small size obliged us to use synchrotron radiation and the new setup developed by Riekel and co-workers at station ID13 at ESRF (Grenoble, France). For its first test, this setup allowed the determination of MIL-110 from a crystal of  $3 \times 3 \times 10 \mu\text{m}$ .<sup>27</sup> The crystal of MIL-100 (Al) with a volume of  $\sim 8 \mu\text{m}^3$  (10 times smaller than MIL-110) gave us the possibility to explore the limits of the setup (see the

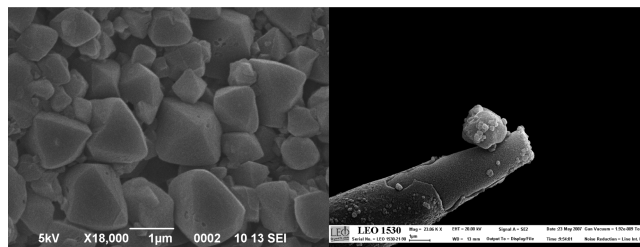


**Figure 1.** SEM images of the aluminum-based MIL-100 (Al) compound showing the typical octahedral shape crystals of 0.5–2  $\mu\text{m}$  length. On the right, a selected crystal of MIL-100 (Al) used for the diffracted intensities collection at station ID13 (ESRF).

Supporting Information). Although the network of MIL-100<sup>6</sup> was previously analyzed with iron or chromium from powder data in combination with computer simulation, the structure presented here was determined for the first time by means of “classical” direct methods and further characterized by solid-state NMR.

The structure of MIL-100 (Al) is built up from the trinuclear octahedrally coordinated aluminum building units, which are arranged in some manner to form a supertetrahedral block (Figure 2). Within this tetrahedral unit, each corner is occupied by the trimeric unit connected to each other through the trimesate ligands located on each face. This  $\{\text{Al}_3\text{O}(\text{OH})(\text{H}_2\text{O})_2\}_4[\text{btc}]_4$  supertetrahedral motif corresponds to an “augmented” version of the  $\text{SiO}_4$  unit encountered in zeolites, and MIL-100 to the “augmented” zeolite ZSM-39,<sup>30</sup> with the MTN<sup>31</sup> topology (Figure 2). The corresponding three-dimensional framework exhibits two types of cavities. The first one is delimited by 12 pentagonal rings defining a dodecahedral cage ( $5^{12}$ , noted S) with window diameter of 5.2 Å. These cages are connected together by sharing 5-ring faces in order to form infinite layers stacked in an ABC sequence. The second cage is generated at the intersection of the rods and delimited by 12 pentagonal rings and 4 hexagonal rings leading to a hexakaidodecahedron cage ( $5^{12}6^4$ , noted L). The L cages are also connected to each other via the hexagonal faces (window diameter of 8.8 Å) with a diamond type. Other MOF-type compounds are also recently reported to adopt such a MTN topology like cadmium-hexamethylenetetramine hybrid<sup>32</sup> or the terbium triazine-1,3,5-tribenzoate.<sup>33</sup>

From the XRD analysis, the MIL-100 structure contains seven nonequivalent crystallographic sites for aluminum that belong to three distinct supertetrahedra, designated from the standard MTN topology T1, T2 and T3 and containing four aluminum trimers. Each trimer is designated  $t_{ijk}$  where  $ijk$  are three aluminum indices (Al<sub>i</sub>Al<sub>j</sub>Al<sub>k</sub>). There are four different trimers,

- (23) Hatop, H.; Ferbinteanu, M.; Roesky, H. W.; Cimpoesu, F.; Schiefer, M.; Schmidt, H.-G.; Noltemeyer, M. *Inorg. Chem.* **2002**, *41*, 1022.  
 (24) Lemoine, P.; Bekaert, A.; Brion, J. D.; Viossat, B. Z. *Kristallogr. NCS* **2006**, *221*, 309.  
 (25) Mueller, U.; Schubert, M.; Teich, F.; Puetter, H.; Schierle-Arndt, K.; Pastré, J. *J. Mater. Chem.* **2006**, *16*, 626.  
 (26) Schubert, M.; Müller, U.; Tonigold, M.; Ruetz, R. Patent WO 2007/023134 A1, **2007**.  
 (27) Volklinger, C.; Popov, D.; Loiseau, T.; Guillou, N.; Férey, G.; Haouas, M.; Taulelle, F.; Mellot-Draznieks, C.; Burghammer, M.; Riekel, C. *Nat. Mater.* **2007**, *6*, 760.  
 (28) Haouas, M.; Volklinger, C.; Loiseau, T.; Férey, G.; Taulelle, F. *Chem.—Eur. J.* **2009**, *15*, 3139.  
 (29) MIL-100 (Al) was synthesized from a mixture of aluminum nitrate (230 mg, 0.61 mmol), trimethyl-1,3,5-trimesate ( $\text{btcMe}_3$ , 104 mg, 0.41 mmol), nitric acid 1 M (0.77 mL, 0.77 mmol), and deionized water (2.8 mL, 155.6 mmol) and placed in a 23 mL Teflon-lined Parr-type autoclave at 210 °C for 3.5 h in an oven (the temperature went up to 210 °C in 1 h). The initial pH was set to 0.57 with an appropriate amount of  $\text{HNO}_3$  and the final pH was measured to 1.77. The resulting yellowish powdered sample was collected by filtration, washed with water, and dried at room temperature.

- (30) Schlenker, J. L.; Dwyer, F. G.; Jenkins, E. E.; Rohrbaugh, W. J.; Kokotailo, G. T. *Nature* **1981**, *294*, 340.  
 (31) Baerlocher, C.; McCusker, L. B.; Olson, D. H. *Atlas of Zeolite Framework Types*, 6th revised ed.; Elsevier: Amsterdam, 2007; p 228.  
 (32) Fang, Q.; Zhu, G.; Xue, M.; Sun, J.; Wei, Y.; Qiu, S.; Xu, R. *Angew. Chem., Int. Ed.* **2005**, *44*, 3845.  
 (33) Park, Y. K.; Choi, S. B.; Kim, H.; Kim, K.; Won, B.-H.; Choi, K.; Choi, J.-S.; Ahn, W.-S.; Won, N.; Kim, S.; Jung, D. H.; Choi, S.-H.; Kim, G.-H.; Cha, S.-S.; Jhon, Y. H.; Yang, J. K.; Kim, J. *Angew. Chem., Int. Ed.* **2007**, *46*, 8230.

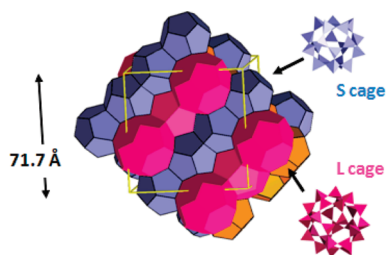


**Figure 2.** Representation of the zeolite MTN topology related to the high silica zeolite ZSM-39, showing the cubic arrangement of the two types of cavities with small (S) cages and large (L) cages.

$t_{111}$ ,  $t_{522}$ ,  $t_{633}$ ,  $t_{744}$ . Therefore, the three distinct super-tetrahedra can be described by their connections to the four trimers constituting its vertices: T1 ( $t_{744} t_{522} t_{522} t_{633}$ ), T2 ( $t_{522} t_{522} t_{522} t_{111}$ ), and T3 ( $t_{111} t_{111} t_{111} t_{111}$ ), with the respective site symmetries  $m$ ,  $3m$ , and  $-43m$ . Each trimer is an augmented realization of the corresponding oxygen atoms of the MTN topology. Their correspondence with the standard notations of the MTN is the following: O1 =  $t_{744}$ , O2 =  $t_{522}$ , O3 =  $t_{633}$ , and O4 =  $t_{111}$ . For each trinuclear building unit, the Al–O distances are typically within the range 1.831(10)–1.995(11) Å. Shorter Al–O distances are observed for the  $\mu_3$ -bridging species within the trimer (1.815(13)–1.875(13) Å) and bond valence calculations<sup>34</sup> suggested the existence of a  $\mu_3$ -oxo ligand (1.78–1.80). Terminal Al–O bonds occur along the axis with the  $\mu_3$ -oxo group within each  $\text{AlO}_6$  octahedron and distances are ranging from 1.894(15) to 2.005(14) Å. From the bond valence calculations, it could correspond to water molecules (0.38–0.52) and hydroxo group (1OH and 2H<sub>2</sub>O per Al trimer) should be present in order to ensure the electroneutrality of the framework. Each of the terminal group also strongly interacts with the water molecules located within the cavities S and L, with typical hydrogen bond distances (2.6–2.9 Å).

The <sup>27</sup>Al MAS NMR spectrum of as-synthesized MIL-100 exhibits in the chemical shift range of –20 to 10 ppm a pattern of overlapped lines (Figure S3, Supporting Information), specifying 6-fold coordination for aluminum sites. The 2D <sup>27</sup>Al MQMAS spectrum (Figure S3a, Supporting Information) indicates that they are composed of three overlapping isotropic resonances with contrasted anisotropic line-shapes due to the difference in quadrupolar coupling. Simulation of the 2D map provided accurate determination of second-order quadrupolar line-shape parameters for all these aluminum sites. They display a very close isotropic chemical shift within the range of 1–3 ppm but different quadrupolar  $C_Q$  varying from 1.3 to 5.6 MHz. The simulation of the anisotropic projection allows to check these parameters, showing an excellent agreement with those from the 2D simulation. Quantitative information is obtained from simulation of the <sup>27</sup>Al 1D spectrum (Figure S3b, Supporting Information) using these parameters. It leads to three components with a relative population ratio of 1.5:10.0:5.4 assigned to Al1, Al2,3,4, and Al5,6,7 sites, respectively, on the basis of their population

ratio of 2:10:5. Two kinds of trimeric units exist:  $t_{111}$  on one hand and  $t_{522}$  or  $t_{633}$  or  $t_{744}$  on the other hand with a multiplicity of 2 and 6 or 3 or 6, respectively. Their relative proportion of 2  $t_{111}$ :15 ( $t_{522}$ ,  $t_{633}$ ,  $t_{744}$ ) provides the expected theoretical multiplicity of 2:10:5 for Al1, Al2,3,4, and Al5,6,7 sites, respectively.

The XRD crystallographic multiplicity of the non-equivalent Al sites respective to Al<sub>i</sub> is 2:4:2:4:2:1:2 for respective Al<sub>i</sub>, and reduces to 2:10:5 classes of NMR nonequivalent aluminum sites meaning the symmetry order is higher for NMR than for XRD. The origin of this higher symmetry stems from protons motion on the framework averaging the different environments by groups, Al1, Al2,3,4, and Al5,6,7 sites, respectively.

The <sup>1</sup>H MAS spectrum (Figure S4a, Supporting Information) shows 3 signals at 4.8, 8.0, and 9.1 ppm assigned to free and bonded water molecules, aromatic protons of extra-lattice trimesic acid H<sub>3</sub>btc entrapped into the pores system, and to aromatic protons of framework trimesate btc. Assignments of the aromatic signals are based on the observation of a substantial decrease in the 8 ppm resonance (about 80%) upon activation. In the <sup>13</sup>C{<sup>1</sup>H} CP MAS spectrum of the activated sample, where almost all trapped organics were removed (Figure S4b, Supporting Information), the overlapped signals in the chemical shifts range of 132–138 ppm are assigned to the aromatic carbons and the resonances at 171 and 172 ppm to the carboxylate groups of framework trimesate btc. Interestingly, the carboxylates signals appeared in a relative proportion of 2:1, respectively. This corresponds to an average btc around a 2 or  $m$  symmetry axis, leading to a 2:1 ratio for every carbon of the btc. Furthermore, the overlapping aromatic signals can be decomposed into 6 components of roughly equal population corresponding to the 6 aromatic carbons, thus supporting distinct crystallographic sites for each carbon in the btc moieties. The carbon atoms can therefore be decomposed into 2 sublattices (carboxyls groups and aromatic ring). It indicates for the former an averaging through protons hopping on the inorganic part of the framework and for the latter, aromatic flipping differentiating all carbons.

Performed on an activated MIL-100 (Al) sample, the thermogravimetric analysis shows two-step weight losses. The first event occurring below 70 °C is assigned to the departure of free water molecules. The second step then corresponds to the removal of the btc ligand (from 370 °C) together with the collapse of the three-dimensional framework. The final product at 520 °C is Al<sub>2</sub>O<sub>3</sub>. The surface area of the activated MIL-100 (Al) was measured to be 2152(39) m<sup>2</sup> g<sup>-1</sup> ( $p/p_0$  range 0.01–0.2 for BET) with a micropore volume of 0.82 cm<sup>3</sup> g<sup>-1</sup> and 2919(44) m<sup>2</sup> g<sup>-1</sup> ( $p/p_0$  range 0.06–0.2 for Langmuir).

**Supporting Information Available:** Experimental details for synthesis, activation procedure, crystallographic and refinement details, solid-state NMR spectroscopy, TGA and BET curves (PDF); CIF file of MIL-100 (Al). This material is available free of charge via the Internet at <http://pubs.acs.org>.

(34) Brese, N. E.; O'Keeffe, M. *Acta Crystallogr., Sect. B* **1991**, *47*, 192.